



# OPEN Photosynthetic responses of *Larix kaempferi* and *Pinus densiflora* seedlings are affected by summer extreme heat rather than by extreme precipitation

Gwang-Jung Kim<sup>1</sup>, Heejae Jo<sup>1</sup>, Min Seok Cho<sup>2,3</sup>, Nam Jin Noh<sup>4</sup>, Seung Hyun Han<sup>2</sup>, Asia Khamzina<sup>1</sup>, Hyung-Sub Kim<sup>1,5</sup> & Yowhan Son<sup>1</sup>✉

The frequency and intensity of summer extreme climate events are increasing over time, and have a substantial negative effect on plants, which may be evident in their impact on photosynthesis. Here, we examined the photosynthetic responses of *Larix kaempferi* and *Pinus densiflora* seedlings to extreme heat (+3 °C and +6 °C), drought, and heavy rainfall by conducting an open-field multifactor experiment. Leaf gas exchange in *L. kaempferi* showed a decreasing trend under increasing temperature, showing a reduction in the stomatal conductance, transpiration rate, and net photosynthetic rate by 135.2%, 102.3%, and 24.8%, respectively, in the +6 °C treatment compared to those in the control. In contrast, *P. densiflora* exhibited a peak function in the stomatal conductance and transpiration rate under +3 °C treatment. Furthermore, both species exhibited increased total chlorophyll contents under extreme heat conditions. However, extreme precipitation had no marked effect on photosynthetic activities, given the overall favorable water availability for plants. These results indicate that while extreme heat generally reduces photosynthesis by triggering stomatal closure under high vapor pressure deficit, plants employ diverse stomatal strategies in response to increasing temperature, which vary among species. Our findings contribute to the understanding of mechanisms underlying the photosynthetic responses of conifer seedlings to summer extreme climate events.

**Keywords** Extreme climate, Multifactor experiment, Gas exchange, Chlorophyll, Larch, Pine

Extreme climate events (e.g., extreme heat, drought, and heavy rainfall), generally defined as inordinately hotter, drier, or wetter conditions compared to the historical reference period, have an increasing trend in terms of frequency, intensity, and magnitude worldwide<sup>1–3</sup>. For example, in Europe, the days of heatwave increased by approximately 71 in 2021 compared to those in the year of 1864, while extreme drought and rainfall increased by approximately six and three times, respectively<sup>4</sup>. Similarly, East Asia also experienced a rise in the frequency of such extreme climate events in recent decades<sup>5</sup>. Moon et al.<sup>6</sup> reported that summer extreme heat and precipitation in East Asia increased by 4–8% over the past three decades. This increase has led to more frequent occurrences of extreme precipitation, culminating in events such as the 2018 Japan flood-heat wave succession<sup>7</sup>. Moreover, numerous studies have reported that these extreme climate events are anticipated to exhibit an increasing trend over time, across various regions<sup>3,8–10</sup>. For instance, if the mean temperature rises by 4.3 °C from the current level, some tropical and subtropical regions could face extreme heat for 15–20% of all days in 2100<sup>8</sup>. Additionally, the frequency of daily 99th percentile of precipitation in Europe is projected to increase by approximately 50% by

<sup>1</sup>Division of Environmental Science and Ecological Engineering, Korea University, 145, Anam-ro, Seongbuk-gu, Seoul 02841, Republic of Korea. <sup>2</sup>Forest Technology and Management Research Center, National Institute of Forest Science, Pocheon 11186, Republic of Korea. <sup>3</sup>Research Planning and Coordination Division, National Institute of Forest Science, Seoul 02455, Republic of Korea. <sup>4</sup>Department of Forest Resources, Kangwon National University, Chuncheon 24341, Republic of Korea. <sup>5</sup>Institute of Life Science and Natural Resources Research, Korea University, Seoul 02841, Republic of Korea. ✉email: yson@korea.ac.kr

2100 compared to 2020<sup>9</sup>. Such extreme climate events can prompt changes in ecosystem functioning and damage the recovery system of plants, thereby inducing irreversible damage<sup>2,11</sup>.

Extreme climate events affect photosynthesis of plants. While photosynthesis typically increases with increasing temperature until an optimum point, extremely high temperature decreases the activity of photosystem II and causes damage to the thylakoid membrane, leading to a substantial reduction in net photosynthetic rate ( $P_n$ )<sup>12,13</sup>. Furthermore, under extreme heat events, the increase in leaf-to-air vapor pressure deficit ( $VPD_L$ ) causes stomatal closure, reducing  $P_n$  and transpiration rate ( $E$ )<sup>14–16</sup>. In extreme drought, reduced soil water availability leads to stomatal closure, limiting transpiration and evaporative cooling<sup>16–18</sup>, thereby pushing plants towards critical temperature thresholds and decreasing chlorophyll content and  $P_n$  due to impaired chloroplast biosynthesis<sup>19</sup>. Although increased soil moisture from rainfall would mitigate these issues, an excessive soil moisture under heavy rainfall leads to soil saturation and flooding, and thus, reduces the availability of oxygen and nutrients to plants, resulting in stomatal closure and degradation of chlorophyll contents and  $P_n$ <sup>20,21</sup>.

The simultaneous extreme climate events pose a greater challenge to the photosynthetic activities of plants than single events<sup>13,16</sup>. For example, during periods of extreme drought, plants experience thermal stresses due to limitations in their ability to cool the leaves through transpiration<sup>22</sup>. This situation can be aggravated with when extreme heat, intensifying the thermal stress to levels that surpass a critical threshold. These hot drought conditions can lead to functional damage and impede the recovery of hydraulic conductance, ultimately increasing the risk of plant mortality<sup>13,23</sup>. It is important to note that hot and humid conditions can also amplify abiotic stresses. The combination of extreme heat and high humidity can lead to a reduction in the biochemical contents (e.g., sucrose, starch, and soluble protein) within leaves, thereby decreasing  $P_n$ <sup>24</sup>. Furthermore, the impact of concurrent extreme climate events during summer, particularly in East Asian monsoon regions, would be exacerbated due to the highest values of both air temperature and precipitation in summer. Despite of the significant impact of combined extreme climate events on photosynthesis, there has been limited focus on them in studies<sup>23,25</sup>.

We selected two conifer species different in plant functional type, *Larix kaempferi* (deciduous) and *Pinus densiflora* (evergreen). Both species are commercially important and widely distributed in South Korea<sup>26,27</sup>. Previous studies have highlighted distinct patterns in the photosynthetic responses of these two species under environmental stress, particularly in terms of hydraulic traits. Bhusal et al.<sup>28</sup> reported that a decrease in leaf water potential and  $P_n$  under water deficit conditions was observed in *L. kaempferi*, but not in *P. densiflora* seedlings in their drought experiment. However, there is lack of previous studies that specifically investigate the photosynthetic activities of these two species in response to extreme heat, either alone or in combination with drought or heavy rainfall. Understanding how extreme conditions impact the photosynthetic activities of seedlings is crucial for anticipating the potential changes in forest ecosystems' function under the increasing frequency of extreme climate events. Therefore, this study aims to investigate the impact of summer extreme heat, drought, and heavy rainfall, as well as their interactions, on the photosynthetic activities of *L. kaempferi* and *P. densiflora* seedlings by examining leaf gas exchange parameters and chlorophyll contents. To achieve the research goals, we simulated extreme climate events in the open field in a manner that mimicked naturally occurring conditions. We formulated the following hypotheses:

- (H1) The extreme heat treatment would decrease  $g_s$  in *L. kaempferi* and *P. densiflora* by inducing stomatal closure under high  $VPD_L$  (H1a), and this decrease would be most pronounced under concurrent drought treatment (H1b). Additionally, the treatments of extreme climate events would decrease chlorophyll contents (H1c).
- (H2) As a consequence of decreased  $g_s$ ,  $E$  and  $P_n$  would decrease under the extreme heat, drought, and heavy rainfall treatments.

## Materials and methods

### Experimental design

The open-field experiment was carried out in Pocheon, South Korea (37° 45' 38.9" N, 127° 10' 13.4" E) (Fig. S1). This site is in the humid continental climate zone, characterized by hot summers and cold/dry winters<sup>29</sup>, with a high inter-annual variation of annual precipitation. Over a period of 23 years (1997–2019), the mean annual temperature at this site ranged from 9.2 to 11.4 °C and the annual precipitation ranged from 870 to 2329 mm.

The experimental setup consisted of six blocks, within each of which nine 1.5 m × 1.0 m plots were established (Fig. S2). Three blocks were assigned for *L. kaempferi* and the remaining three blocks were designated for *P. densiflora*. Within each plot, a random combination of two types of treatments was assigned: temperature treatments (ambient, ambient + 3 °C, and ambient + 6 °C; referred to as TC, T3, and T6, respectively) and precipitation treatments (ambient, complete exclusion of rainfall as extreme drought, and water addition above the ambient as heavy rainfall; referred to as PC, DR, and HR, respectively). Two factorial combinations were introduced, consisting of three temperature regimes and three precipitation regimes. Consequently, 54 plots were arrayed at the experimental site (two species × three temperature levels × three precipitation levels × three replicates). In April 2020, a total of 88 and 99 1-year-old *L. kaempferi* and *P. densiflora* seedlings, respectively, were planted in each plot following the guidelines for seedling management provided by Korea Forest Service (2020). The soil texture at the experimental site was classified as sandy loam (70% sand, 20% silt, and 10% clay).

Infrared heaters (FT-1000, Mor Electronic Heating Assoc., Comstock Park, MI, USA) were used to increase the canopy temperature (CT) in the T3 and T6 treatments (Fig. S4). Infrared thermometers (SI-111, Apogee Instruments, Logan, UT, USA) measured the CT of experimental plots, and dataloggers (CR1000X, Campbell Scientific, Inc., Logan, UT, USA) and relays (SDM-CD-16AC, Campbell Scientific, Logan, UT, USA) maintained the target temperature under the T3 and T6 treatments (if CT reached the target temperature, relays switched off

the heaters). To monitor soil temperature (ST) and SWC, measurements were taken at a depth of 5 cm using a soil temperature/moisture sensor (SI-111, Campbell Scientific, Logan, UT, USA). An automatic rainout shelter with a transparent roof (2.0 m × 1.5 m) intercepted the natural rainfall in DR plots. The rainout shelter would close only when a rain detector (HTL-301, Haimil, Republic of Korea) detected rainfall, in order to avoid disturbance from the microclimate (e.g., light and airflow) within the plots. For the HR treatment, an artificial rainfall simulator was used. This simulator employed two spray nozzles (Unijet D5-35, Spraying Systems Co., Wheaton, IL, USA) per plot, spraying water stored in a tank. For more detailed information on the experimental design, please refer to Fig. S3 and the study conducted by Kim et al.<sup>30</sup>.

To determine the threshold and establish the experimental scenario of extreme climate events, we utilized meteorological data from the reference period of 1961–2019 for the months of July and August in Seoul. Since meteorological data for the research site were available only after 1997, we used the data from the nearest city, Seoul, located approximately 30 km away, as a reference (Fig. S1). The target temperatures of T3 and T6 were determined based on the difference between the mean daily maximum temperature (29.9 °C) and the 90th (33.2 °C) and 99th (36.0 °C) percentiles of the daily maximum temperature, respectively, during the reference period<sup>1</sup>. The duration of the extreme heat treatment was determined as the longest period of consecutive days with a daily maximum temperature above the threshold for extreme heat during the reference period, which was determined to be 7 days. For DR, it was defined as the longest period of consecutive days with daily precipitation of less than 1 mm during the reference period, which amounted to 9 days<sup>31</sup>. HR was defined as the 95th percentile of the daily precipitation during the reference period, which amounted to 113 mm day<sup>-1</sup><sup>32</sup>. To determine the duration of HR, we calculated the longest consecutive period with daily precipitation exceeding the threshold of heavy rainfall, which was set at 3 days.

We simulated these extreme climate events from July–August 2020. The manipulation of temperature and precipitation was divided into two periods, with one-week of no treatment period in-between the treatment periods. The first and second DR treatments were applied on the 195–203 and 218–226 day of the year (DOY), respectively. However, during the second period, soil water content (SWC) in DR plots unexpectedly increased due to naturally occurring heavy rainfall on DOY 213–217, 219, and 222. HR was implemented on DOY 197, 200, and 203 during the first period, and on DOY 220, 223, and 226 during the second period. Temperature manipulation was carried out on DOY 204–210 and DOY 227–233.

### Measurement of photosynthetic parameters

During the experimental period of July–August 2020, in situ measurements of leaf gas exchange of *L. kaempferi* and *P. densiflora* seedlings were performed using a portable photosynthesis system (LI-6800, Li-Cor Inc., Lincoln, NE, USA) with a 3 cm × 3 cm chamber (6800-12A, Li-Cor Inc., Lincoln, NE, USA). Leaf gas exchange measurements were conducted five times throughout the experimental period. The measurements were carried out on the needles of three randomly selected seedlings per each plot. The measurements were taken at a photosynthetic photon flux density of 1000 μmol m<sup>-2</sup> s<sup>-1</sup>, relative humidity of 50%, CO<sub>2</sub> concentration of 400 μmol mol<sup>-1</sup>, and an ambient air temperature ranging from 27 to 33 °C. Consistent with the experimental design, gas exchange measurements were conducted between 0900 and 1500 h to minimize any diurnal variations. After field measurements were conducted, the needles were brought to the lab, where their area was determined using a scanner (Perfection V700 Photo, EPSON, Japan) and an image analysis system (WinSEEDLE, Regent Instruments Inc., Québec City, QC, Canada). This information was used to calculate the measured values of  $P_n$ ,  $E$ ,  $g_s$ , and the ratio of intercellular to ambient CO<sub>2</sub> concentration ( $C_i/C_a$ ) on a leaf area basis. Additionally, water use efficiency (WUE) and intrinsic water use efficiency (iWUE) were calculated using the ratios of  $P_n/E$  and  $P_n/g_s$ , respectively.

To measure the chlorophyll content, the needles were cut to a length of approximately 2 mm. Subsequently, 20 ± 1 mg of cut needles were placed into vials containing 5 mL of dimethyl sulfoxide (DMSO). The vials were then incubated at 65 °C for 6 h in a water bath (HQ-DW22, Coretech Korea Co., Republic of Korea) to extract the chlorophyll. After the incubation period, the absorbance of the chlorophyll extracts was measured at 648 nm and 665 nm using a spectrophotometer (UH5300, Hitachi, Japan). The absorbance values at these wavelengths were used to calculate the chlorophyll a (Chl<sub>a</sub>), chlorophyll b (Chl<sub>b</sub>), and total chlorophyll (Chl<sub>t</sub>) contents using the following equations<sup>33</sup>:

$$\text{Chl}_a = (14.84 \times A_{665} - 5.14 \times A_{648}) \times V \div \text{F.W.} \quad (1)$$

$$\text{Chl}_b = (25.48 \times A_{648} - 7.36 \times A_{665}) \times V \div \text{F.W.} \quad (2)$$

$$\text{Chl}_t = (7.49 \times A_{665} - 20.34 \times A_{648}) \times V \div \text{F.W.} \quad (3)$$

where  $A_{665}$  and  $A_{648}$  are the absorbances at 665 nm and 648 nm, respectively.  $V$  is the volume of DMSO, and F.W. is the fresh weight of needles.

To calculate VPD<sub>L</sub>, we derived hourly air temperature and relative humidity from the automatic weather station at the experimental site. The leaf temperature for VPD<sub>L</sub> calculation was obtained from the infrared thermometer in the plots. VPD<sub>L</sub> was calculated based on air saturation vapor pressure (ASVP) and leaf saturation vapor pressure (LSVP) using the following equations<sup>14,34</sup>:

$$\text{ASVP} = 610.78 \times e^{[T_{\text{air}}/(T_{\text{air}}+237.3) \times 17.2694]} \quad (4)$$

$$\text{LSVP} = 610.78 \times e^{[T_{\text{leaf}}/(T_{\text{leaf}}+237.3) \times 17.2694]} \quad (5)$$

$$\text{VPD}_L = \text{LSVP} - (\text{ASVP} \times \text{RH}/100) \quad (6)$$

where  $T_{\text{air}}$  and  $T_{\text{leaf}}$  are the air and leaf temperatures, respectively, and RH is relative humidity. We assumed that all plots were under the equivalent RH, considering that the experiment was conducted in an open field<sup>35</sup>.

### Data analysis

The effects of temperature and precipitation manipulation on the environmental factors were examined using repeated measures analysis of variance (ANOVA). Additionally, the effects of temperature and precipitation manipulation on the  $\text{VPD}_L$ , leaf gas exchange, and chlorophyll content were determined by two-way ANOVA using a linear mixed model to account for a randomized complete block design. The block was treated as a random effect and the temperature and precipitation treatments were treated as fixed effects. The linear mixed model equation used for analysis is as follows:

$$Y_{ijkl} = \beta_0 + \beta_1 T_j + \beta_2 P_k + \beta_3 TP_{ijk} + \varepsilon_l + \varepsilon_{ijkl} \quad (7)$$

where  $Y_{ijkl}$  is the response variable in the  $i$ th observation ( $i = 1-5$ ) under  $j$ th temperature treatment  $T$  ( $j = \text{TC}, \text{T3}, \text{or T6}$ ) and  $k$ th precipitation treatment  $P$  ( $k = \text{PC}, \text{DR}, \text{or HR}$ ) with  $l$ th block ( $l = 1-3$ ).  $TP$  is the interaction between  $T$  and  $P$ ,  $\beta_0$  is the intercept,  $\beta_n$  are coefficients to be estimated ( $n = 1-3$ ),  $\varepsilon_k$  is the random residuals associated with the block, and  $\varepsilon_{ijkl}$  is the final residuals. As coefficients of  $P$  and  $TP$  were not statistically significant for all photosynthetic parameters ( $P > 0.05$ ), the variables were removed from the analysis. In addition, due to an increase in SWC in the DR treatment during the second period, caused by naturally occurring heavy rainfall, we excluded the data on photosynthetic activities measured during and following this period from the analysis. We verified the statistically significant differences among precipitation treatments within temperature treatments via Tukey's post hoc test.

The effect size for each parameter was calculated as the natural logarithm of the response ratio (RR) to compare the means of treatment (T3, T6, DR, or HR) with the means of control (TC or PC) by the following equation<sup>36</sup>:

$$\text{RR} = \ln(\bar{X}_t/\bar{X}_c) \quad (8)$$

where  $\bar{X}_t$  and  $\bar{X}_c$  are the means of parameters in the temperature and precipitation treatment and control, respectively. The variance ( $v$ ) of RR was calculated as:

$$v = \frac{(SD_t)^2}{n_t \bar{X}_t} + \frac{(SD_c)^2}{n_c \bar{X}_c} \quad (9)$$

where  $SD_t$  and  $SD_c$  are the standard deviation of parameters in the treatment and control, respectively, and  $n_t$  and  $n_c$  are the sample sizes of parameters in the treatment and control, respectively. The statistical significance between the treatment and control was determined by Tukey's post hoc test.

The relationships among  $\text{VPD}_L$ ,  $E$ ,  $C_i/C_a$ , and  $P_n$  with  $g_s$  were examined by non-linear regression. Specifically, the relationship between  $\text{VPD}_L$  and  $g_s$  was determined using the equation proposed by Oren et al.<sup>37</sup>:

$$g_s = -m \times \ln(\text{VPD}_L) + b \quad (10)$$

where  $m$  represents the slope and  $b$  represents a reference  $g_s$  at  $\text{VPD}_L = 1$  kPa.

Principal component analysis (PCA) was carried out to determine the relationships among environmental factors and photosynthetic activities. All data analyses and visualizations were conducted with R version 4.2.1 at a significance level of 0.05<sup>38</sup>. R packages of "lme4" for linear mixed model<sup>39</sup>, "sjstats" for RR<sup>40</sup>, and "ggplot2" for data visualization<sup>41</sup> were used.

### Research ethics

The experimental research on *L. kaempferi* and *P. densiflora* seedlings, including the collection of seedling material, complied with relevant institutional, national, and international guidelines and legislation. As the seedlings were cultivated and maintained by the National Institute of Forest Science, a joint research institute involved in this study, no specific permissions were required for the seedling collection.

## Results

### Environmental conditions

CT during the temperature manipulation period was significantly different among TC, T3, and T6 ( $P < 0.001$ ) (Fig. 1a). The mean CT during the first temperature manipulation period was 2.6 °C and 5.8 °C higher in T3 and T6, respectively, compared to that in TC. During the second period, the mean CT in T3 and T6 was also significantly higher (2.6 °C and 5.7 °C) than that in TC, respectively ( $P < 0.001$ ). Temperature manipulation also significantly affected ST during both temperature manipulations ( $P < 0.001$ ) (Fig. 1b). The mean ST (°C ± one standard error) was 22.7 ± 1.0, 24.5 ± 1.2, and 26.3 ± 1.8 in TC, T3, and T6, respectively, during the first temperature manipulation period. During the second period, ST was 26.0 ± 0.4, 27.3 ± 0.5, and 28.9 ± 0.9 in TC, T3, and T6, respectively.

There was no significant effect of temperature manipulation on SWC ( $P = 0.59$ ) (Fig. 1c). Precipitation manipulation significantly affected SWC during the first manipulation period ( $P < 0.001$ ). The mean SWC (vol. %) during this period was 7.8 ± 2.2, 10.1 ± 2.0, and 12.2 ± 2.1 in DR, PC, and HR, respectively. The difference in SWC among treatments during the second manipulation was also statistically significant ( $P = 0.04$ ). The mean

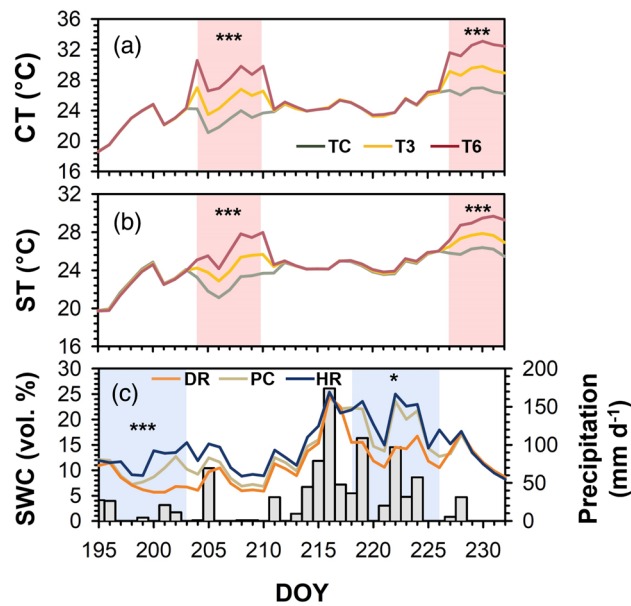


**Figure 1.** Canopy temperature (CT) (a), soil temperature (ST) (b), and soil water content (SWC) (c) and daily precipitation (gray bars) during the experimental period. Red and blue areas mean the period of temperature and precipitation manipulation, respectively. TC: temperature control; T3: +3 °C treatment; T6: +6 °C treatment; DR: extreme drought; PC: precipitation control; HR: heavy rainfall treatment. Asterisks depict statistical differences among TC, T3, and T6 in CT and ST, and DR, PC, and HR in SWC (\* $P < 0.05$ ; \*\* $P < 0.01$ ; \*\*\* $P < 0.001$ ). DOY means day of the year. This figure was modified from Kim et al.<sup>30</sup>.

SWC was higher than that in the earlier manipulation, measuring  $13.6 \pm 2.3$ ,  $18.4 \pm 4.4$ , and  $20.3 \pm 7.1$  in DR, PC, and HR, respectively.

### Leaf gas exchange and chlorophyll content

The  $VPD_L$  significantly increased with increased temperature in both *L. kaempferi* and *P. densiflora* ( $P < 0.001$ ) (Fig. 2a,b).  $VPD_L$  ranged between 1.10–1.67 kPa in *L. kaempferi* and 1.11–1.70 kPa in *P. densiflora*.  $g_s$  significantly decreased as  $VPD_L$  increased in *L. kaempferi* ( $P < 0.001$ ) (Fig. 2c), whereas there was no significant correlation between  $g_s$  and  $VPD_L$  in *P. densiflora* ( $P = 0.37$ ) (Fig. 2d).

Temperature manipulation significantly affected  $g_s$ ,  $E$ ,  $C_i/C_a$ ,  $P_n$ , WUE, and iWUE of *L. kaempferi* (Figs. 3a–d, 4a,b) and  $g_s$ ,  $E$ , and  $C_i/C_a$  of *P. densiflora* (Fig. 3e–g), whereas precipitation manipulation and the interaction between the two treatments did not exhibit an overall effect (Figs. 3a–h, 4a–d, 5b,d; Table 1). Under T3,  $g_s$ ,  $E$ , and  $C_i/C_a$  in *L. kaempferi* experienced a decrease, with effect sizes of  $-0.37 \pm 0.10$  ( $P < 0.01$ ),  $-0.26 \pm 0.10$  ( $P = 0.02$ ), and  $-0.06 \pm 0.01$  ( $P < 0.01$ ), respectively (Fig. 5a), whereas those in *P. densiflora* increased with effect sizes of  $0.36 \pm 0.15$  ( $P = 0.01$ ),  $0.23 \pm 0.13$  ( $P = 0.07$ ), and  $0.01 \pm 0.01$  ( $P = 0.48$ ), respectively (Fig. 5c). The reductions in  $g_s$ ,  $E$ , and  $C_i/C_a$  in *L. kaempferi* were more pronounced under T6, with effect sizes of  $-0.86 \pm 0.15$  ( $P < 0.001$ ),  $-0.70 \pm 0.14$  ( $P < 0.001$ ), and  $-0.11 \pm 0.02$  ( $P < 0.001$ ), respectively, while only  $C_i/C_a$  in *P. densiflora* decreased under T6 ( $P < 0.001$ ). In addition,  $E$ ,  $C_i/C_a$ , and  $P_n$  exhibited an increasing trend with increased  $g_s$  in *L. kaempferi* ( $P < 0.001$ ) (Fig. 6a–c). However, only  $E$  and  $C_i/C_a$  were positively correlated with  $g_s$  in *P. densiflora* ( $P < 0.001$ ) (Fig. 6d,e), while the relationship between  $P_n$  and  $g_s$  was not statistically significant ( $P = 0.38$ ) (Fig. 6f).

$Chl_a$  and  $Chl_t$  in both *L. kaempferi* and *P. densiflora* were higher in warmer plots, whereas precipitation manipulation did not have a significant impact on chlorophyll content (Table 2). In *L. kaempferi*, the effect size on  $Chl_a$  and  $Chl_t$  in T3 was  $0.26 \pm 0.06$  ( $P < 0.001$ ) and  $0.21 \pm 0.07$  ( $P < 0.001$ ), respectively, while in T6 it was  $0.26 \pm 0.08$  ( $P < 0.001$ ) and  $0.24 \pm 0.09$  ( $P < 0.001$ ), respectively (Fig. 5a). For *P. densiflora*, the effect size on  $Chl_a$  and  $Chl_t$  were  $0.08 \pm 0.06$  ( $P = 0.48$ ) and  $-0.04 \pm 0.07$  ( $P = 0.06$ ), respectively, in T3, while it was  $0.22 \pm 0.07$  ( $P = 0.02$ ) and  $0.20 \pm 0.07$  ( $P = 0.02$ ), respectively, in T6 (Fig. 5c).

By analyzing all photosynthetic parameters and environmental factors with PCA, the biplot of *L. kaempferi* showed a definite grouping by temperature treatments (Fig. 7a). PC1 of *L. kaempferi* explained 56.38% of the variations and indicated that  $E$ ,  $g_s$ , and  $C_i/C_a$  were negatively related to CT, WUE, and iWUE. PC2 explained 14.54% of the total variations and indicated the positive correlation among  $P_n$ ,  $Chl_t$ , CT, and ST. The results of PCA for *P. densiflora* seedlings showed that PC1 and PC2 explained 54.30% and 17.61% of the total variations, respectively (Fig. 7b). PC1 revealed that  $E$  and  $C_i/C_a$  were negatively related to the WUE and iWUE of *P. densiflora* and PC2 explained the relationship among environmental factors.

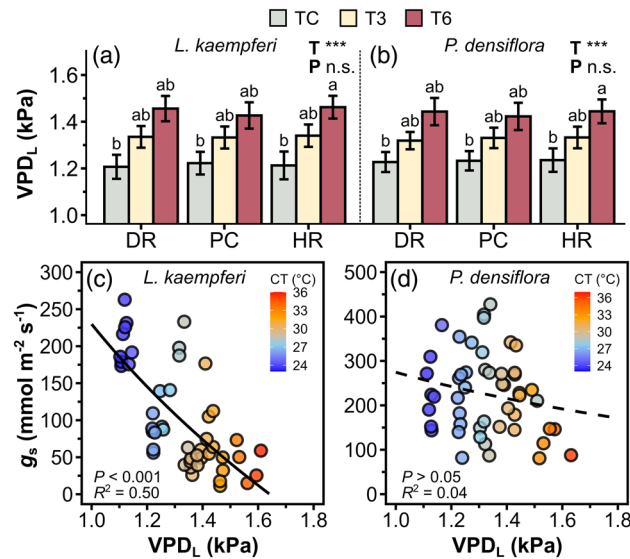


**Figure 2.** Leaf-to-air vapor pressure deficit ( $VPD_L$ ) of *Larix kaempferi* (a) and *Pinus densiflora* (b) seedlings under temperature (T) and precipitation (P) manipulation, and stomatal conductance ( $g_s$ ) as a function of  $VPD_L$  of *L. kaempferi* (c) and *P. densiflora* (d) seedlings. Gray, yellow, and red-colored bars indicate the temperature control (TC), +3 °C treatment (T3), and +6 °C treatment (T6), respectively. Colors of points are represented by canopy temperature (CT). Solid and dashed line represent the significant and non-significant regression, respectively. The regression equations are as follows:  $Y = -463.49 \times \ln(X) + 229.84$  (*L. kaempferi*);  $Y = -175.73 \times \ln(X) + 274.51$  (*P. densiflora*). Asterisks show the level of significance (n.s.: non-significant, \* $P < 0.05$ ; \*\* $P < 0.01$ ; \*\*\* $P < 0.001$ ). DR: extreme drought; PC: precipitation control; HR: heavy rainfall treatment.

## Discussion

The functionality of temperature and precipitation manipulation systems is crucial when conducting experiments in the open field, as ambient climate factors can easily influence the experimental treatments<sup>2</sup>. In this study, the temperature manipulation system successfully simulated the conditions of real extreme heat events. The temperature manipulation system ensured that the heated and ambient plots had distinct CT and ST conditions, even during periods of rainfall (DOY 205 and 228) or under extremely high air temperature (33.1 °C on DOY 232; data not shown) conditions. However, there was an unexpected increase in SWC in DR plots during the second manipulation period. These results were inconsistent with those that would occur under water stress, and we propose that the cause of the increased SWC was the naturally occurring extreme precipitation events. Specifically, during the rest period between the two periods of experimental precipitation manipulation, the study area received a significant amount of rainfall (358 mm) over a five-day period (DOY 213–217), which accounted for 26% of the mean annual precipitation over 23 years. It is suggested that the rainfall may have entered the plots through open sides, resulting in an increase in SWC in DR plots. These unexpected results emphasize a limitation commonly associated with the open-field experiment. Thus, we suggest considering the edge part of the plots as a buffer zone to minimize the potential influence of ambient factors, such as lateral influx of rainfall or microclimate variations when conducting the open-field experiment.

Consistent with our hypothesis (H1a), as the temperatures increased,  $g_s$  in *L. kaempferi* showed a decreasing trend (Fig. 3a). This result is consistent with the concept that high temperatures can lead to stomatal closure in order to mitigate water loss<sup>14,42</sup>. Elevated evaporative demand and subsequent leaf water loss associated with high temperatures may also contribute to stomatal closure<sup>18,43</sup>. The significant negative relationship between  $g_s$  and  $VPD_L$  in *L. kaempferi* found in this study was supported by these established theories (Fig. 2c). This decreasing trend in  $g_s$  under high temperatures and  $VPD_L$  confirms the findings of a previous study by Amey et al.<sup>44</sup> wherein the photosynthetic responses of *P. taeda* seedlings were examined under experimental heat waves with a biweekly +6 °C treatment. The closure of stomata is likely responsible for the reduction in  $E$  and  $C_i/C_a$ <sup>14,15,45,46</sup>. In our study, the positive relations observed between  $E$ ,  $C_i/C_a$ , and  $g_s$  in *L. kaempferi* as well as PCA results provide further evidence that the decrease in  $E$  and  $C_i/C_a$  is associated with stomatal closure, thus in line with H2. The decrease in  $CO_2$  uptake can lead to oxidative damage and a decline in  $P_n$ <sup>47,48</sup>. Additionally, heat stress may inhibit the  $CO_2$  fixation of plants and damage components of their photosynthetic apparatus, especially photosystem II, which plays a crucial role in electron transport during photosynthesis, as leaf temperature increases<sup>47</sup>. However, in our study,  $P_n$  of *L. kaempferi* significantly decreased only under T6, but not under T3. This result suggests that the relatively lower  $VPD_L$  under T3, compared to T6, was not sufficient to inhibit  $P_n$ , since the sensitivity of  $P_n$  to  $VPD_L$  is weaker than that of  $g_s$ <sup>14</sup>.

In contrast to *L. kaempferi*, the increasing  $VPD_L$  did not have a significant impact on  $g_s$  of *P. densiflora* (Fig. 2d). Furthermore,  $g_s$  and  $E$  of *P. densiflora* increased under T3 and decreased again in T6 (Fig. 5c). These results are contrary to H1a, suggesting species-specific variation of stomatal behaviors in responses to temperature and  $VPD_L$ . The observed peak responses of  $g_s$  and  $E$  to increasing  $VPD_L$  and temperature can be interpreted as a

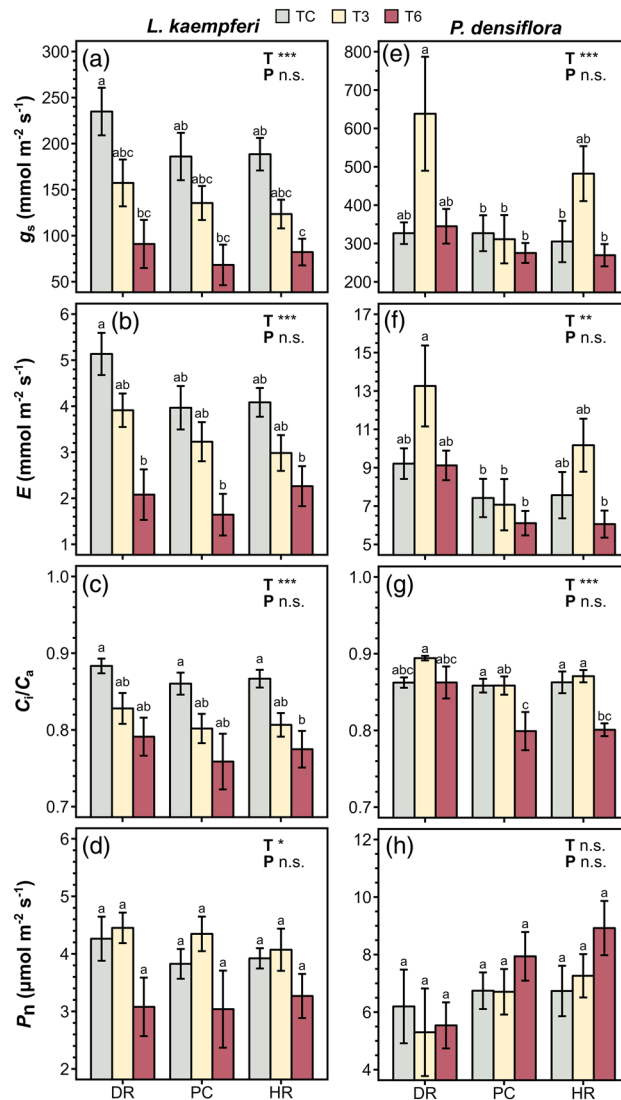


**Figure 3.** Stomatal conductance ( $g_s$ ), transpiration rate ( $E$ ), ratio of intercellular to ambient  $\text{CO}_2$  concentration ( $C_i/C_a$ ), and net photosynthetic rate ( $P_n$ ) of *Larix kaempferi* (a–d, respectively) and *Pinus densiflora* (e–h, respectively) seedlings under temperature (T) and precipitation (P) manipulation. Gray, yellow, and red-colored bars indicate the temperature control (TC), +3 °C treatment (T3), and +6 °C treatment (T6), respectively. Vertical lines represent one standard error of the means. Asterisks show the level of significance (n.s.: non-significant, \* $P < 0.05$ ; \*\* $P < 0.01$ ; \*\*\* $P < 0.001$ ). Different letters above the bars depict the significant differences among treatments. DR Extreme drought, PC Precipitation control, HR Heavy rainfall treatment.

trade-off between the ‘feed-back’ and ‘feed-forward’ stomatal responses. Stomatal transpiration can increase as a strategy for cooling the leaf surface under high temperatures, representing a feed-back response<sup>49</sup>. Conversely, a feed-forward response involves a decline in  $E$  as temperature and  $\text{VPD}_L$  increase to avoid hydraulic failure<sup>43,50</sup>. During the feed-back response, the evaporative cooling strategy may induce water loss through the leaf cuticle. Subsequently,  $g_s$  and  $E$  may begin to decrease after reaching a certain level of  $\text{VPD}_L$  and temperature in response to this water loss, aiming to prevent hydraulic failure, thus exhibiting a peak function<sup>14,51,52</sup>. Although these peaked responses have been a subject of debate as it is difficult to explain the response from simple stomatal mechanisms, previous studies have suggested that there is an optimum  $\text{VPD}_L$  and temperature for  $E$ <sup>51</sup>. Furthermore, previous findings have observed that these responses are more likely to occur when temperature co-varies with  $\text{VPD}_L$ , rather than when temperature remains constant. The observed peaked response of  $g_s$  and  $E$  of *P. densiflora* under the extreme heat treatment can be interpreted as a result of the trade-off between the evaporative cooling and minimizing water loss, particularly given the covariation of temperature and  $\text{VPD}_L$  in our experiment.

These divergent stomatal strategies in response to extreme heat may be attributed to differences in the species’ hydraulic traits<sup>14</sup>. Specifically, the high sensitivity of  $g_s$  to  $\text{VPD}_L$  in *L. kaempferi* suggests an isohydric behavior. In contrast, *P. densiflora* appeared to withstand the extreme heat stress through anisohydric stomatal regulation, as evidenced by its consistent  $P_n$  under the treatments. In addition, the distinction in needle morphology could

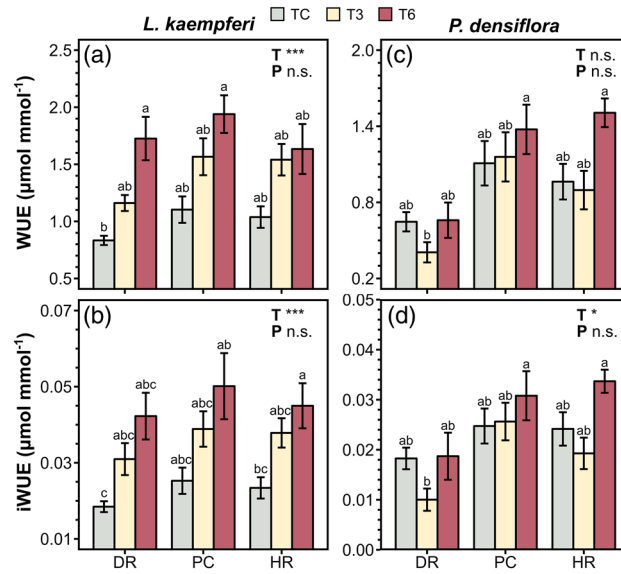


**Figure 4.** Water use efficiency (WUE) and intrinsic WUE (iWUE) of *Larix kaempferi* (a, b, respectively) and *Pinus densiflora* (c, d, respectively) seedlings under temperature (T) and precipitation (P) manipulation. Gray, yellow, and red-colored bars indicate the temperature control (TC), +3 °C treatment (T3), and +6 °C treatment (T6), respectively. Vertical lines represent one standard error of the means. Asterisks show the level of significance (n.s.: non-significant, \* $P < 0.05$ ; \*\* $P < 0.01$ ; \*\*\* $P < 0.001$ ). Different letters above the bars depict the significant differences among treatments. DR Extreme drought, PC Precipitation control, HR Heavy rainfall treatment.

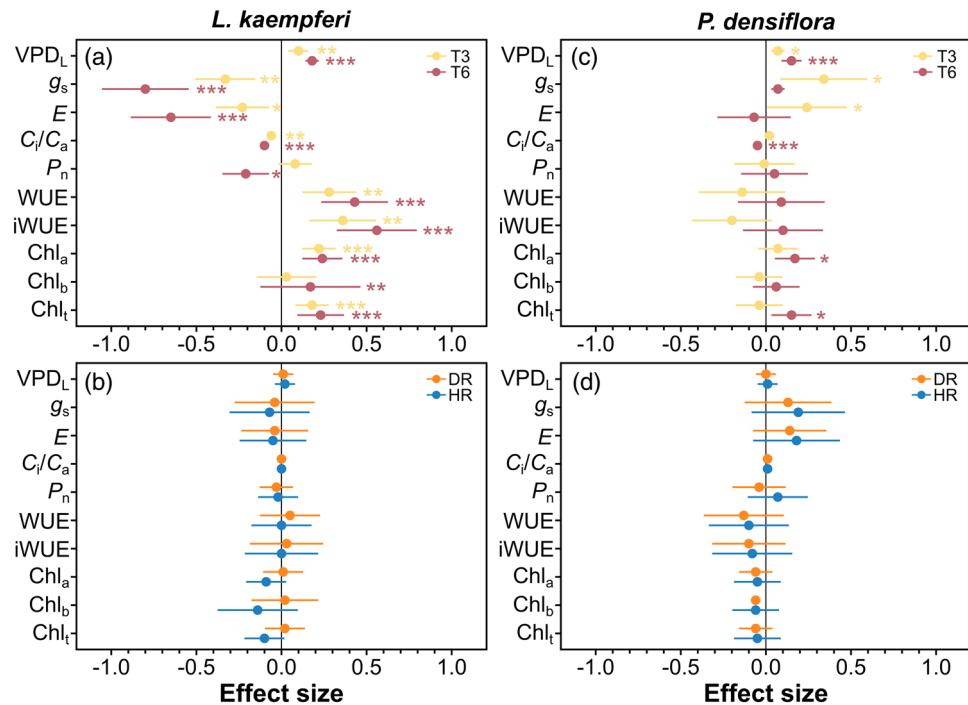


**Figure 5.** The effect size of photosynthetic parameters of *Larix kaempferi* (a, b) and *Pinus densiflora* (c, d) seedlings. Yellow and red colored-symbols indicate the +3 °C treatment (T3) and +6 °C treatment (T6), respectively, and orange and blue-colored symbols indicate the extreme drought (DR) and heavy rainfall (HR) treatment. Horizontal lines represent one standard error. Asterisks show the significant differences to the control (\* $P < 0.05$ ; \*\* $P < 0.01$ ; \*\*\* $P < 0.001$ ).



Species	Effect	d.f	VPD <sub>L</sub>	g <sub>s</sub>	E	C <sub>i</sub> /C <sub>a</sub>	P <sub>n</sub>	WUE	iWUE	Chl <sub>a</sub>	Chl <sub>b</sub>	Chl <sub>t</sub>
<i>Larix kaempferi</i>	T	2	14.70***	13.08***	10.69***	12.71***	3.70*	11.81***	12.35***	7.49**	0.55	5.01**
	P	2	0.03	0.59	0.48	0.19	0.18	0.01	0.18	1.95	0.42	1.57
	T×P	4	0.06	0.53	0.63	0.15	0.26	0.24	0.16	0.62	0.45	0.50
<i>Pinus densiflora</i>	T	2	13.29***	7.01**	5.58**	11.12***	0.69	2.44	3.80*	7.64**	1.80	6.62**
	P	2	0.03	0.08	0.13	0.32	1.06	0.24	0.31	0.22	0.17	0.22
	T×P	4	0.03	2.08	1.69	1.18	0.35	0.49	0.67	0.70	1.70	0.87

**Table 1.** Summary (*F* values) of two-way ANOVA for leaf-to-air vapor pressure deficit (VPD<sub>L</sub>) and photosynthetic responses of *Larix kaempferi* and *Pinus densiflora* seedlings to temperature and precipitation manipulation. Asterisks show the significant differences to the control (\**P* < 0.05; \*\**P* < 0.01; \*\*\**P* < 0.05). VPD<sub>L</sub>, Leaf-to-air vapor pressure deficit; g<sub>s</sub>, Stomatal conductance; E, Transpiration rate; C<sub>i</sub>/C<sub>a</sub>, Ratio of intercellular to ambient CO<sub>2</sub> concentration; P<sub>n</sub>, Net photosynthetic rate; WUE, Water use efficiency; iWUE, Intrinsic water use efficiency; Chl<sub>a</sub>, Chlorophyll a content; Chl<sub>b</sub>, Chlorophyll b content; Chl<sub>t</sub>, Total chlorophyll content.

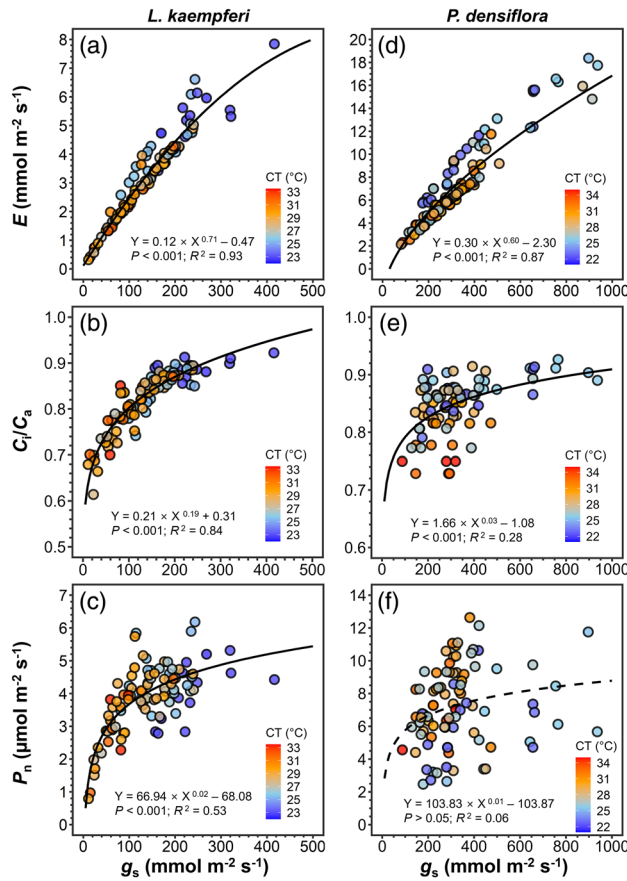


**Figure 6.** Transpiration rate (*E*), ratio of intercellular to ambient CO<sub>2</sub> concentration (*C<sub>i</sub>/C<sub>a</sub>*), and net photosynthetic rate (*P<sub>n</sub>*) as a function of stomatal conductance (*g<sub>s</sub>*) of *Larix kaempferi* (a–c) and *Pinus densiflora* (d–f) seedlings under temperature and precipitation manipulation. Colors of points are represented by canopy temperature (CT). Solid and dashed lines represent the significant and non-significant regressions, respectively.

contribute to variation in stomatal behaviors between the two species. Longer needles are likely to receive a higher irradiance on their surface, resulting high requirement for CO<sub>2</sub> uptake, compared to shorter needles<sup>53,54</sup>. This demand is met through increased leaf hydraulic conductance, *g<sub>s</sub>*, and evaporative demand. Furthermore, longer needles possess a higher hydraulic capacity, essential for delivering the water needed to maintain open stomata<sup>53</sup>. These hydraulic traits of a long leaf are evidenced by higher values of *g<sub>s</sub>*, *E*, and *P<sub>n</sub>*, and feed-back stomatal response in *P. densiflora* in this study which has a longer needle (approximately 5.93 ± 0.23 cm needle<sup>-1</sup>) compared to *L. kaempferi* (approximately 2.31 ± 0.05 cm needle<sup>-1</sup>). Additionally, the evergreen characteristics of *P. densiflora* likely contribute to the differential stomatal behavior, as evergreen species may invest more in carbon uptake due to their longer leaf lifespan, in contrast to deciduous species such as *L. kaempferi*, which

Species	Manipulation		Chlorophyll contents (mg g <sup>-1</sup> )		
	Temperature	Precipitation	Chl <sub>a</sub>	Chl <sub>b</sub>	Chl <sub>t</sub>
<i>Larix kaempferi</i>	TC	DR	0.69 (0.02) ab	0.16 (0.01) a	0.85 (0.03) ab
		PC	0.66 (0.05) ab	0.17 (0.02) a	0.83 (0.08) ab
		HR	0.52 (0.03) b	0.15 (0.02) a	0.66 (0.05) b
	T3	DR	0.80 (0.05) ab	0.20 (0.04) a	1.01 (0.09) ab
		PC	0.80 (0.06) a	0.16 (0.02) a	0.96 (0.07) a
		HR	0.75 (0.05) a	0.15 (0.01) a	0.90 (0.06) ab
	T6	DR	0.77 (0.09) ab	0.17 (0.03) a	0.94 (0.12) ab
		PC	0.85 (0.15) ab	0.21 (0.02) a	1.06 (0.16) ab
		HR	0.77 (0.05) ab	0.18 (0.06) a	0.95 (0.09) ab
<i>Pinus densiflora</i>	TC	DR	0.66 (0.00) c	0.12 (0.01) b	0.78 (0.01) c
		PC	0.93 (0.04) abc	0.21 (0.01) a	1.14 (0.05) abc
		HR	0.76 (0.07) bc	0.16 (0.02) ab	0.92 (0.09) bc
	T3	DR	0.76 (0.06) bc	0.14 (0.00) ab	0.90 (0.05) bc
		PC	0.96 (0.11) abc	0.18 (0.02) ab	1.13 (0.13) abc
		HR	0.92 (0.06) abc	0.18 (0.01) ab	1.10 (0.07) abc
	T6	DR	0.82 (0.01) abc	0.17 (0.01) ab	0.98 (0.02) abc
		PC	1.10 (0.09) ab	0.20 (0.02) ab	1.30 (0.10) ab
		HR	1.15 (0.11) a	0.22 (0.02) a	1.37 (0.13) a

**Table 2.** Mean (SE) chlorophyll contents of *Larix kaempferi* and *Pinus densiflora* seedlings under temperature and precipitation manipulation. Chl<sub>a</sub>, Chlorophyll a content; Chl<sub>b</sub>, Chlorophyll b content; Chl<sub>t</sub>, Total chlorophyll content; TC, Temperature control; T3, + 3 °C Treatment; T6, + 6 °C Treatment; DR, Drought treatment; PC, Precipitation control; HR, Heavy rainfall treatment. Different letters mean the statistical significance among treatments.

have ‘disposable’ leaves<sup>55</sup>. The distinct hydraulic regulations might be a critical factor in plant mortality under environmental stresses<sup>56</sup>. Anisohydric behavior may provide short-term tolerance to heat stresses, as observed in our study. However, the prolonged hot and dry conditions can rapidly lead anisohydric species to dehydration and xylem cavitation, ultimately resulting in mortality due to their increased  $E$  at high temperatures<sup>16</sup>. Therefore, examining photosynthetic activities under long-term environmental stresses is essential for predicting plant survival following extreme climate events.

Interestingly,  $P_n$  in *P. densiflora* did not show changes with increasing temperature and there was no observed correlation between  $P_n$  and  $g_s$  (Figs. 3h, 6f). These findings suggest that  $P_n$  in *P. densiflora* may be influenced by factors other than  $g_s$ , indicating a more complex relationship between stomatal behavior and photosynthetic performance. A study by Urban et al.<sup>22</sup> examining gas exchange variables in responses to increasing temperature in *P. taeda* and *Populus deltoides* × *nigra* also observed the decoupled relationship between  $g_s$  and  $P_n$  at leaf temperatures > 40 °C, further supporting the complex interactions between these variables. In addition, a peak response of  $g_s$  to increasing VPD<sub>l</sub> was likely a contributing factor to the decoupling between  $g_s$  and  $P_n$ <sup>57</sup>. These results highlight the need for further research to explore underlying mechanisms influencing  $P_n$  in *P. densiflora* and to elucidate the factors that contribute to its photosynthetic response under extreme temperature conditions.

Contrary to our hypothesis (H1c), our study found markedly high chlorophyll contents under the extreme heat treatment for both *L. kaempferi* and *P. densiflora*. While chlorophyll contents generally tend to decrease under thermal stress due to leaf senescence, there may exist an optimal temperature range where chlorophyll contents can increase as temperature rises. Previous studies have found that high temperatures may enhance plant growth and accelerate pigment biosynthesis, and the activity of enzymes involved in chlorophyll production, resulting in an increase in chlorophyll contents<sup>58,59</sup>. However, upon examining the growth and biomass data from the current study (data not shown), the temperature treatments did not have an impact on seedling growth and biomass in either species. Seedling height (cm) and total biomass (g seedling<sup>-1</sup>) of *L. kaempferi* and *P. densiflora* were not affected by the temperature treatment ( $P=0.27$  and  $0.88$ , respectively, for *L. kaempferi*; Noh et al.<sup>26</sup>, and  $P=0.61$  and  $0.85$ , respectively, for *P. densiflora*; unpublished data), ranging from 48.6–57.5 and 13.24–15.88, respectively, in *L. kaempferi*, and from 28.6–29.7 and 6.89–7.96, respectively, in *P. densiflora*. Consequently, the increased chlorophyll contents in the extreme heat treatment might be attributed to the accelerated pigment biosynthesis rather than the enhanced growth of seedlings. Yun et al.<sup>27</sup> also observed that Chl<sub>t</sub> in *P. densiflora* increased within the air temperature range of 15–31 °C in their experiment, where an increase in air temperature by 3 °C was simulated using the infrared heater. In our study, the observed high chlorophyll contents under extreme heat, with CT ranging from 24 to 32 °C, suggest that this temperature range may correspond to the optimum conditions for pigment biosynthesis.

In general, water deficit conditions typically lead to stomatal closure and a reduction in CO<sub>2</sub> uptake, thereby reducing  $g_s$ ,  $E$ , and  $P_n$ <sup>60,61</sup>. However, in this study, we did not observe a decrease in photosynthetic parameters under DR in both *L. kaempferi* and *P. densiflora* (Fig. 5b,d). This result could be attributed to the brief duration of summer drought spells experienced in the East Asian monsoon climate of the study region. While the lack of



## Conclusion

To summarize, we found that *L. kaempferi* showed a decrease in  $g_s$  under extreme heat, leading to the reduction in all photosynthetic parameters, whereas *P. densiflora* showed a peak function in  $g_s$  and  $E$  under extreme heat and no change in  $P_n$ . No effect was observed of extreme drought and heavy rainfall on photosynthetic activities in both species. These findings reveal the species differences in stomatal behaviors in response to increasing temperature and *L. kaempferi* experiencing more pronounced adverse effects on photosynthesis compared to *P. densiflora*. These results indicate that extreme heat may have a more negative impact on forest succession dynamics and degrade ecosystems' function in newly established *L. kaempferi* forests, by inhibiting carbon uptake, in comparison to *P. densiflora* forests. Therefore, these findings suggest the significance of implementing temperature management strategies in nursery systems, particularly for *L. kaempferi*, to effectively respond to extreme climate events. However, we note that the observed responses spanned only a single season, whereas experimental treatments in open-field trials can be inferred by natural environmental stochasticity, necessitating a long-term study. Thus, further long-term studies are needed to assess the lagged effect of summer extreme conditions in subsequent seasons and the recovery capacity of plants from extreme climate events.

## Data availability

The data that support the findings of this study can be obtained from the corresponding author upon reasonable request.

Received: 3 July 2023; Accepted: 29 February 2024

Published online: 04 March 2024

## References

- Alexander, L. V. *et al.* Global observed changes in daily climate extremes of temperature and precipitation. *J Geophys Res Atmospheres* **1984** *2012* **111**, D05109 (2006).
- Jentsch, A., Kreyling, J. & Beierkuhnlein, C. A new generation of climate-change experiments: Events, not trends. *Front. Ecol. Environ.* **5**, 365–374 (2007).
- Shenoy, S., Gorinevsky, D., Trenberth, K. E. & Chu, S. Trends of extreme US weather events in the changing climate. *Proc National Acad Sci* **119**, e2207536119 (2022).
- Espinosa, L. A., Portela, M. M., Matos, J. P. & Gharbia, S. Climate change trends in a European coastal metropolitan area: Rainfall, temperature, and extreme events (1864–2021). *Atmosphere* **13**, 1995 (2022).
- World Meteorology Organization *State of the climate in Asia 2021*. (2022).
- Moon, J.-Y., Choi, Y., Kim, Y. & Min, S. Subseasonal to annual long-term trends in climate extremes over East Asia, 1981–2021. *Front. Earth Sci.* **10**, 880462 (2022).
- Wang, S. S.-Y. *et al.* Consecutive extreme flooding and heat wave in Japan: Are they becoming a norm? *Atmos. Sci. Lett.* **20**, (2019).
- Zeppetello, L. R. V., Raftery, A. E. & Battisti, D. S. Probabilistic projections of increased heat stress driven by climate change. *Commun. Earth Environ.* **3**, 183 (2022).
- Myhre, G. *et al.* Frequency of extreme precipitation increases extensively with event rareness under global warming. *Sci. Rep.* **9**, 16063 (2019).
- Freychet, N., Hegerl, G., Mitchell, D. & Collins, M. Future changes in the frequency of temperature extremes may be underestimated in tropical and subtropical regions. *Commun. Earth Environ.* **2**, 28 (2021).
- Ruehr, N. K., Grote, R., Mayr, S. & Arneith, A. Beyond the extreme: Recovery of carbon and water relations in woody plants following heat and drought stress. *Tree Physiol.* **39**, 1285–1299 (2019).
- Hozain, M. I., Salvucci, M. E., Fokar, M. & Holaday, A. S. The differential response of photosynthesis to high temperature for a boreal and temperate *Populus* species relates to differences in Rubisco activation and Rubisco activase properties. *Tree Physiol.* **30**, 32–44 (2010).
- Teskey, R. *et al.* Responses of tree species to heat waves and extreme heat events. *Plant Cell Environ.* **38**, 1699–1712 (2015).
- Grossiord, C. *et al.* Plant responses to rising vapor pressure deficit. *New Phytol.* **226**, 1550–1566 (2020).
- Haworth, M. *et al.* The impact of heat stress and water deficit on the photosynthetic and stomatal physiology of olive (*Olea europaea* L.)—A case study of the 2017 heat wave. *Plants* **7**, 76 (2018).
- Marchin, R. M. *et al.* Extreme heat increases stomatal conductance and drought-induced mortality risk in vulnerable plant species. *Global Change Biol.* **28**, 1133–1146 (2022).
- Limousin, J.-M. *et al.* Regulation and acclimation of leaf gas exchange in a piñon–juniper woodland exposed to three different precipitation regimes. *Plant Cell Environ.* **36**, 1812–1825 (2013).
- Kolb, P. F. & Robberecht, R. High temperature and drought stress effects on survival of *Pinus ponderosa* seedlings. *Tree Physiol.* **16**, 665–672 (1996).
- Bhusal, N., Lee, M., Han, A. R., Han, A. & Kim, H. S. Responses to drought stress in *Prunus sargentii* and *Larix kaempferi* seedlings using morphological and physiological parameters. *Forest Ecol. Manag.* **465**, 118099 (2020).
- Li, L. *et al.* Ecological responses to heavy rainfall depend on seasonal timing and multi-year recurrence. *New Phytol.* **223**, 647–660 (2019).
- Chen, H., Qualls, R. G. & Blank, R. R. Effect of soil flooding on photosynthesis, carbohydrate partitioning and nutrient uptake in the invasive exotic *Lepidium latifolium*. *Aquat. Bot.* **82**, 250–268 (2005).
- Urban, J., Ingwers, M. W., McGuire, M. A. & Teskey, R. O. Increase in leaf temperature opens stomata and decouples net photosynthesis from stomatal conductance in *Pinus taeda* and *Populus deltoides* x *nigra*. *J. Exp. Bot.* **68**, 1757–1767 (2017).
- Rehnschuh, R. & Ruehr, N. K. Diverging responses of water and carbon relations during and after heat and hot drought stress in *Pinus sylvestris*. *Tree Physiol.* **42**, 1532–1548 (2021).
- Wei, J. *et al.* Quantitative proteomic, physiological and biochemical analysis of cotyledon, embryo, leaf and pod reveals the effects of high temperature and humidity stress on seed vigor formation in soybean. *Bmc Plant Biol.* **20**, 127 (2020).
- Bauweraerts, I. *et al.* The effect of heat waves, elevated [CO<sub>2</sub>] and low soil water availability on northern red oak (*Quercus rubra* L.) seedlings. *Glob. Chang. Biology* **19**, 517–528 (2013).
- Noh, N.-J., Kim, G.-J., Son, Y. & Cho, M.-S. Early growth responses of *Larix kaempferi* (Lamb.) Carr. seedling to short-term extreme climate events in summer. *Forests* **12**, 1595 (2021).
- Yun, S. J. *et al.* Short-term effects of warming treatment and precipitation manipulation on the ecophysiological responses of *Pinus densiflora* seedlings. *Turk. J. Agric. For.* **40**, 621–630 (2016).
- Bhusal, N. *et al.* Evaluation of morphological, physiological, and biochemical traits for assessing drought resistance in eleven tree species. *Sci. Total Environ.* **779**, 146466 (2021).

29. Kottek, M., Grieser, J., Beck, C., Rudolf, B. & Rubel, F. World Map of the Köppen-Geiger climate classification updated. *Meteorol. Z.* **15**, 259–263 (2006).
30. Kim, G.-J. *et al.* Experimental design of open-field temperature and precipitation manipulation system to simulate summer extreme climate events for plants and soils. *Turk. J. Agric. For.* **47**, 132–142 (2023).
31. Grant, K., Kreyling, J., Heilmeyer, H., Beierkuhnlein, C. & Jentsch, A. Extreme weather events and plant–plant interactions: shifts between competition and facilitation among grassland species in the face of drought and heavy rainfall. *Ecol. Res.* **29**, 991–1001 (2014).
32. Pendergrass, A. G. What precipitation is extreme?. *Science* **360**, 1072–1073 (2018).
33. Barnes, J. D., Balaguer, L., Manrique, E., Elvira, S. & Davison, A. W. A reappraisal of the use of DMSO for the extraction and determination of chlorophylls a and b in lichens and higher plants. *Environ. Exp. Bot.* **32**, 85–100 (1992).
34. Dai, Z., Edwards, G. E. & Ku, M. S. B. Control of photosynthesis and stomatal conductance in *Ricinus communis* L. (castor bean) by leaf to air vapor pressure deficit. *Plant Physiol.* **99**, 1426–1434 (1992).
35. Kreyling, J. *et al.* Drought effects in climate change manipulation experiments: Quantifying the influence of ambient weather conditions and rain-out shelter artifacts. *Ecosystems* **20**, 301–315 (2017).
36. Hedges, L. V., Gurevitch, J. & Curtis, P. S. The meta-analysis of response ratios in experimental ecology. *Ecology* **80**, 1150–1156 (1999).
37. Oren, R. *et al.* Survey and synthesis of intra- and interspecific variation in stomatal sensitivity to vapour pressure deficit. *Plant Cell Environ.* **22**, 1515–1526 (1999).
38. R Core Team. R: A language and environment for statistical computing. (2022).
39. Bates, D., Mächler, M., Bolker, B. & Walker, S. Fitting linear mixed-effects models using lme4. *J. Stat. Softw.* **67**, (2015).
40. Lüdecke, D. sjstats: Statistical functions for regression models. (0.17.2). *Zenodo* (2018).
41. Wickham, H. ggplot2, elegant graphics for data analysis. (2009) doi:<https://doi.org/10.1007/978-0-387-98141-3>.
42. Running, S. W. Environmental control of leaf water conductance in conifers. *Can. J. Forest Res.* **6**, 104–112 (1976).
43. Farquhar, G. Feedforward responses of stomata to humidity. *Func. Plant Biol.* **5**, 787–800 (1978).
44. Ameje, M. *et al.* The effect of induced heat waves on *Pinus taeda* and *Quercus rubra* seedlings in ambient and elevated CO<sub>2</sub> atmospheres. *New Phytol.* **196**, 448–461 (2012).
45. Guerrieri, R. *et al.* Disentangling the role of photosynthesis and stomatal conductance on rising forest water-use efficiency. *Proc. National Acad. Sci.* **116**, 16909–16914 (2019).
46. Tominaga, J., Shimada, H. & Kawamitsu, Y. Direct measurement of intercellular CO<sub>2</sub> concentration in a gas-exchange system resolves overestimation using the standard method. *J. Exp. Bot.* **69**, 1981–1991 (2018).
47. Hussain, S. *et al.* Photosynthesis research under climate change. *Photosynth. Res.* **150**, 5–19 (2021).
48. Kumari, V. V. *et al.* Drought and heat stress in cool-season food legumes in sub-tropical regions: Consequences, adaptation, and mitigation strategies. *Plants* **10**, 1038 (2021).
49. Sadok, W., Lopez, J. R. & Smith, K. P. Transpiration increases under high-temperature stress: Potential mechanisms, trade-offs and prospects for crop resilience in a warming world. *Plant Cell Environ.* **44**, 2102–2116 (2021).
50. Franks, P. J., Cowan, I. R. & Farquhar, G. D. The apparent feedforward response of stomata to air vapour pressure deficit: information revealed by different experimental procedures with two rainforest trees. *Plant, Cell Environ.* **20**, 142–145 (1997).
51. Duursma, R. A. *et al.* The peaked response of transpiration rate to vapour pressure deficit in field conditions can be explained by the temperature optimum of photosynthesis. *Agr. Forest Meteorol.* **189**, 2–10 (2014).
52. Henry, C. *et al.* A stomatal safety-efficiency trade-off constrains responses to leaf dehydration. *Nat. Commun.* **10**, 3398 (2019).
53. Wang, N., Palmroth, S., Maier, C. A., Domec, J. & Oren, R. Anatomical changes with needle length are correlated with leaf structural and physiological traits across five *Pinus* species. *Plant, Cell Environ.* **42**, 1690–1704 (2019).
54. Brodribb, T. J., Feild, T. S. & Jordan, G. J. Leaf maximum photosynthetic rate and venation are linked by hydraulics. *Plant Physiol.* **144**, 1890–1898 (2007).
55. Wright, I. J. *et al.* The worldwide leaf economics spectrum. *Nature* **428**, 821–827 (2004).
56. Hu, Y. *et al.* Tree-level stomatal regulation is more closely related to xylem hydraulic traits than to leaf photosynthetic traits across diverse tree species. *Agric. For. Meteorol.* **329**, 109291 (2023).
57. Marchin, R. M., Medlyn, B. E., Tjoelker, M. G. & Ellsworth, D. S. Decoupling between stomatal conductance and photosynthesis occurs under extreme heat in broadleaf tree species regardless of water access. *Glob. Chang. Biol.* **29**, 6319–6335 (2023).
58. Ormrod, D. P., Lesser, V. M., Olszyk, D. M. & Tingey, D. T. Elevated temperature and carbon dioxide affect chlorophylls and carotenoids in Douglas-fir seedlings. *Int. J. Plant Sci.* **160**, 529–534 (1999).
59. Rastogi, A. *et al.* Impact of warming and reduced precipitation on morphology and chlorophyll concentration in peat mosses (*Sphagnum angustifolium* and *S. fallax*). *Sci. Rep.* **10**, 8592 (2020).
60. Gao, R., Shi, X. & Wang, J. R. Comparative studies of the response of larch and birch seedlings from two origins to water deficit. *New Zeal. J. For. Sci.* **47**, 14 (2017).
61. Llorens, L. *et al.* Effects of an experimental increase of temperature and drought on the photosynthetic performance of two *Ericaceae* shrub species along a north–south European gradient. *Ecosystems* **7**, 613–624 (2004).
62. an irrigation experiment. Lopez C, M. L. *et al.* Effect of increased rainfall on water dynamics of larch (*Larix cajanderi*) forest in permafrost regions, Russia. *J. Forest. Res.* **15**, 365–373 (2010).
63. Jo, H., Noulékoun, F., Khamzina, A., Chang, H. & Son, Y. Physiological and shoot growth responses of *Abies holophylla* and *Abies koreana* seedlings to open-field experimental warming and increased precipitation. *Water* **14**, 356 (2022).
64. Meissner, R., Seeger, J. & Rupp, H. Lysimeter studies in East Germany concerning the influence of set aside of intensively farmed land on the seepage water quality. *Agric., Ecosyst. Environ.* **67**, 161–173 (1998).

## Author contributions

G.-J.K., H.J., M.S.C., N.J.N., and Y.S. conceptualized the project. G.-J.K., M.S.C., N.J.N., and S.H.H. conducted the experiment and collected data. M.S.C., S.H.H., and Y.S. supervised the project. G.-J.K. analyzed the results and drafted the manuscript. A.K. and H.-S.K. helped with data analysis and interpretation of results. All authors discussed the results and contributed to the final manuscript.

## Funding

This study was carried out with the support of ‘R&D Program for Forest Science Technology (Project No. “2020181A00-2222-BB01”)’ provided by Korea Forest Service (Korea Forestry Promotion Institute), Core Research Institute Basic Science Research Program through the National Research Foundation of Korea (NRF) funded by the Ministry of Education (Project No. NRF-2021R1A6A1A10045235), the National Institute of Forest Science (Grant No. SC0300-2023-01), the Graduate School Specialized in Carbon Sink provided by Korea Forest Service (Korea Forestry Promotion Institute), Korea Environment Industry & Technology Institute (KEITI) through “Climate Change R&D Project for New Climate Regime (RS-2022-KE002294)”, funded by Korea

Ministry of Environment (MOE), the Ministry of Land, Infrastructure, and Transport and the Korea Agency for Infrastructure Technology Advancement (23UMRG-B158194-04), and a Korea University Grant (2023).

### Competing interests

The authors declare no competing interests.

### Additional information

**Supplementary Information** The online version contains supplementary material available at <https://doi.org/10.1038/s41598-024-56120-3>.

**Correspondence** and requests for materials should be addressed to Y.S.

**Reprints and permissions information** is available at [www.nature.com/reprints](http://www.nature.com/reprints).

**Publisher's note** Springer Nature remains neutral with regard to jurisdictional claims in published maps and institutional affiliations.



**Open Access** This article is licensed under a Creative Commons Attribution 4.0 International License, which permits use, sharing, adaptation, distribution and reproduction in any medium or format, as long as you give appropriate credit to the original author(s) and the source, provide a link to the Creative Commons licence, and indicate if changes were made. The images or other third party material in this article are included in the article's Creative Commons licence, unless indicated otherwise in a credit line to the material. If material is not included in the article's Creative Commons licence and your intended use is not permitted by statutory regulation or exceeds the permitted use, you will need to obtain permission directly from the copyright holder. To view a copy of this licence, visit <http://creativecommons.org/licenses/by/4.0/>.

© The Author(s) 2024